Available online at www.sciencedirect.com
ScienceDirect
Energy Procedia 49 (2014) 705 – 714
Energy Procedia

SolarPACES 2013

A regenerative heat storage system for central receiver technology working with atmospheric air

Antonio L. Avila-Marin[a,*], Monica Alvarez-Lara[a], Jesus Fernandez-Reche[b]

[a]*Plataforma Solar de Almeria – CIEMAT, Avda. Complutense 40, Madrid E-28040, Spain*
[b]*Plataforma Solar de Almeria – CIEMAT, P.O. Box 22,Tabernas-Almeria E-04200, Spain*

Abstract

Solar thermal power plants (STPP) are focused on reducing costs while increasing performance. In this context central receiver (CR) technology working with volumetric receiver shows a high potential to improve efficiencies by allowing higher operating temperatures. This technology requires the implementation of efficient thermal energy storage (TES) that allows predictable electricity delivery to the grid. Moreover, to compete with the advantage of molten salt technology storage, the CR technology based in air as heat transfer fluid (HTF) must identify TES solutions that enable efficient thermal storage times, that could be considered dispatchable, and competitive specific costs under 20 €/kWh_{th}. It may be considered that the reference solution for thermal storage in STPP-CR with open volumetric receiver continues being the TSA project developments, also adopted in the experimental plant in Jülich.

Knowing the present market situation, CIEMAT-PSA developed a lab-scale packed bed storage system, with the main objective of identifying economically competitive materials and configurations for efficient regenerative heat storage. For the newer configurations, CIEMAT-PSA has 4-Al_2O_3 commercial balls with two diameters – 9 and 13 mm –, and two densities – 2.3 and 3.5 g/cm^3 – that allows different configurations to be analyzed.

Dynamics tests with 9 mm Al_2O_3 balls and 2.3 g/cm^3 have been carried out for air inlet temperatures near 400ºC until 640ºC.

In addition, a simplified dynamic model, whose formulation is widely assumed in the literature as reasonable to represent the realistic thermal performance, will be used, in order to compare the experimental and predicted temperature profiles, during the charging process.

Selection and peer review by the scientific conference committee of SolarPACES 2013 under responsibility of PSE AG.
Final manuscript published as received without editorial corrections.

* Corresponding author. Tel.: +34-913466629.
E-mail address: antonio.avila@ciemat.es.

Selection and peer review by the scientific conference committee of SolarPACES 2013 under responsibility of PSE AG.
Final manuscript published as received without editorial corrections.
doi:10.1016/j.egypro.2014.03.076

Keywords: Thermocline; packed bed; storage; alumina; air; central receiver;

1. Introduction

Solar energy is not available constantly producing a net electrical output in inherent state of change. Moreover, the energy demand of most domestic and industrial applications is also time dependent while the time of need normally differs from the solar energy supply. Consequently, power plants needs may require a functional low-cost storage of energy to mitigate the changes in solar radiation, to meet portions of these energy needs or demand peaks.

STPP with power tower technology based on air-cooled receivers are a promising technology, with a simpler design, operational advantages, the potential for high conversion efficiencies and on the verge of commercial receiver development [1]. This opens up good opportunities for a rapid market introduction. Commercial implementation of power tower technology with open volumetric receiver depends among other factors on cost-effective large-scale solutions for heat storage. It may be considered that the reference solution for thermal energy storage continues being the TSA project tested at PSA in 1991. It consisted of a 2.5 MW_{th} volumetric air receiver together with a thermal storage and steam generator. However, rather than aspects of storage design, the system demonstration was in the focus of work. The storage was based on a packed bed of aluminum oxide in spherical shape, providing a thermal capacity of about 1 MWh. The tested concept showed a fully functional behavior although this system did not allow a direct scale-up to commercial size: high costs, in the order of 140 €/kWh_{th} [2], for the high-purity aluminium oxide and increased thermally-induced mechanical loads during cyclic operation represent the main barriers [3]. The heat storage of the Jülich power tower plant [4] uses refractory in a stacked arrangement and therefore avoids such mechanical issues.

This type of technology is based on sensible heat storage where thermal energy can be stored by rising or dropping of temperatures of thermal storage media. The thermal energy stored in a mass of material can be expressed as [5]:

$$Q = \rho \cdot V \cdot \bar{c}_p \cdot \Delta T \tag{1}$$

For a material to be useful in a TES application, it must have good thermal capacity, $\rho \cdot \bar{c}_p$, and be cheap enough. Another important parameter in sensible TES is the thermal diffusivity [5] that point out the rate at which the heat can be released and extracted. Table 1 shows the main characteristics of the most commonly-used solid thermal storage materials [5, 6] for medium to high temperature SHS applications.

Table 1. Solid-state sensible heat storage materials [5-6]

Storage materials	Working temperature (ºC)	Density (kg/m^3)	Thermal conductivity (W/m/K)	Specific heat (kJ/kg/K)	Volume expansion (10^{-6}/K)	Specific heat ($kWh^{th}/m^3/K$)
Cast steel	200–700	7800	40.0	0.60	-	1.30
Silica fire bricks	200–700	1820	1.5	1.00	-	0.51
Magnesia fire bricks	200–1200	3000	5.0	1.15	-	0.96
Alumina (99.5%)	> 750	3960	35.0	0.80	16.2	0.88
Cast iron (BS grade 3D)	> 750	7800	-	0.54	32.4	1.17
High alumina concrete	> 750	2400	-	0.98	43.5	0.65
Graphite (pure)	> 750	2230	-	0.71	23.7	0.44
Magnesia (hot pressed)	> 750	3565	-	0.94	24	0.93
Silicon carbide (hot pressed, commercial purity)	> 750	3210	-	1.04	13.2	0.93

Regenerative heat storage provides a considerable design freedom and flexibility that is to be investigated [3]. One of the targets to be studied is the implementation of economically competitive materials and configurations for efficient heat storage [7]. Therefore, CIEMAT-PSA has developed a lab-scale packed bed system as experimental facility. This system could be operated in static and dynamic configuration. For the first one, the experimental loop allows the characterization of effective thermo-physical parameters of the bed, material thermal conductivity, thermal losses, stored energy, etc. for different filler materials while the second allows a quite-agile characterization of the global storage at different working temperatures, filler materials, charges and discharges strategies, etc.

As a result, the main goal for this experimental capability is to analyze the feasibility of different materials as heat storage for the packed beds, attempting to find economical materials that match the required thermal properties. For large storage systems, specific costs for the storage sub-system under 20 €/kWh$_{th}$ [8-9] seems to be possible in a near future contrasting with the original 140 €/kWh$_{th}$ in the Phoebus-TSA study [2]. And at the same time, it will allow us to model the thermal behavior of this storage.

For the thermal verification of the packed bed, the testing facility is going to be operated with four different alumina spheres, as it was the reference filler material used in the TSA project for the air technology verification. Table 2 depicts the commercial characteristics and the expected energy density. It is expected to analyzed further materials for comparison with the ones presented in this paper.

Table 2. Commercial alumina spheres characteristics

Material	Size (mm)	Density (kg/m^3)	Color	Expected energy density (kWh/m^3)	Filler material cost ($/kg)
Alumina (70%)	9 / 13	2300	Light yellow	380	1.3
Alumina (99%)	9 / 13	3500	Pure white	580	1.6

This paper presents the dynamic results for 9 mm alumina spheres with 70% purity. The next experimentation steps will analyze the remaining filler materials, after an improvement in the hot air extraction system. The tests were divided in two phases:

- First, the thermal behavior of the tank was analyzed for an air inlet temperature nearly 600ºC and different mass flow rates.
- Second, the thermal behavior of the tank was analyzed for one mass flow rate and different air inlet temperatures.

Moreover, a mathematical equation that describes the behavior of the packed bed is presented.

Nomenclature

CR	Central receiver
HTF	Heat transfer fluid
SHS	Sensible heat storage
STTP	Solar thermal power plants
TES	Thermal energy storage
a	Ratio between thermal losses area and tank volume, 1/m
c_p	Specific heat, J/kg/K
D	Filler material mean diameter, m
G	Mass velocity per unit area, kg/ m^2/s
h	Inter phase heat transfer coefficient, W/m^2/K
h_v	Volumetric heat transfer coefficient, W/m^3/K
k	Thermal conductivity, W/m/K
P	Perimeter, m
R	Filler material mean radius, m
t	Time, s
T	Temperature, K

u	Velocity of the fluid, m/s
U	Global losses coefficient, $W/m^2/K$
x	Thickness, m
ρ	Density, kg/m^3
ε	Porosity, -

Subscripts

amb	Ambient
eff	Effective
f	Fluid
s	Solid
th	Thermal

2. Experimental TES system prototype

The experimental packed bed TES prototype designed by CIEMAT-PSA is composed by an insulated stainless steel vessel filled with 0.1 m^3 of 70% alumina spheres with 9 mm diameter. Fig. 1 shows the TES in static configuration and the vessel filled with alumina spheres, before the lid application.

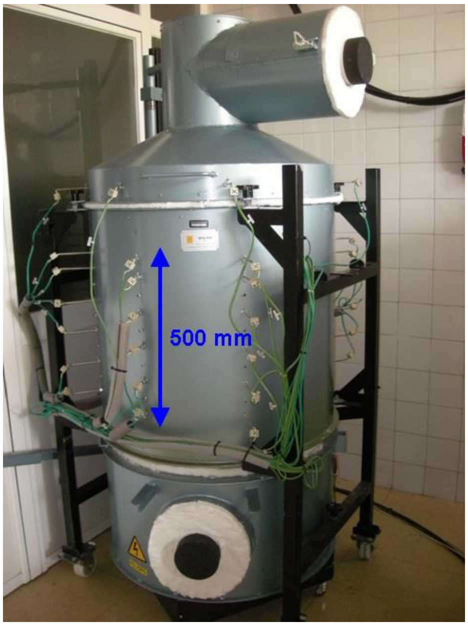

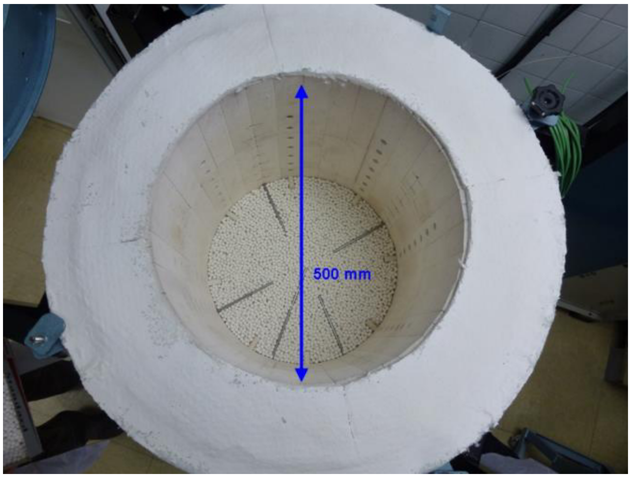

Fig. 1. Packed bed in static arrangement (left), Vessel with thermocouples distribution inside the filler material (right)

The packed system is equipped with 35 K-type thermocouples units of 400 mm long located at 7 levels with 5 measurements each level. At each level, the thermocouples record the internal temperature during the test at different depths. Moreover, 5 PT100 surface sensors record the external temperature of the packed bed, for the thermal losses evaluation.

Air is the fluid that carries the energy and circulates through the packed bed delivering or recovering the energy. There are two possible circulations through the tank, charging or discharging. During the charging process, hot air circulates from the top to the bottom of the tank delivering the energy to the solid media. During the discharging process, the fluid flow is the opposite, and cold air (ambient or exhaust air) is pumped through the packed bed from the bottom to the top of the tank leaving the tank at a higher temperature, recovering the thermal energy previously transferred. The flow direction is important since, for the single-tank TES system concept, thermal stratification is achieved and maintained over the time exploiting the buoyancy effect of the air contained into the storage [10].

In order to simulate the solar radiation absorbed by the volumetric receiver, the hot air is provided by a 15 kW electric heater. For the evaluation of the thermal efficiency during the charging/discharging steps, the total electrical energy consumption is registered.

The tests carried out are summarized in Table 3: test 1-to-4 for an air inlet temperature of approximately 570ºC and four different mass flow rates, and test 5-to-8 for an almost constant air mass flow rates, in between 63-69 kg/h, and four different air inlet temperatures.

Table 3. Tests carried out at constant air inlet temperature (1-4) and constant mass flow rate (5-8)

Test	1	2	3	4	5	6	7	8
T_{air_inlet}, (ºC)	570	570	570	570	430	500	570	640
m, (kg/h)	38	54	66	75	69	69	66	63

3. Thermal evaluation and model description

Various charging tests for different mass flow rates and air inlet temperatures, with 9 mm 70 % alumina spheres, have been performed to check the thermal behavior of the TES prototype. During the tests the mass flow rate was not measured directly. An indirect measurement was calculated with the information of the heater power and the induced temperature increment, as follows:

$$\dot{m} = \frac{Power}{c_{p_{air}} \cdot \Delta T} \tag{2}$$

The instantaneous amount of energy stored in the packed bed during the process has been calculated to study the thermal efficiency during charging/discharging processes. The expression used for the energy calculation is:

$$Q_{stored} = \dot{m} \cdot c_{p_{air}} \cdot \Delta t \cdot \left(T_{in,\tan k} - T_{out,\tan k}\right) \tag{3}$$

Finally, for the evaluation of the material thermal behavior, the charging efficiency was computed as the ratio between the total stored energy in the tank and the total energy consumption during the process.

$$\eta_{ch\arg ing} = \frac{\int_{t_0}^{t_{end}} Q_{stored} \cdot dt}{E_{consumption}} \tag{4}$$

Model the behavior of the tank, based on the experimental data, is an important tool to predict the performance of the tank under different conditions or even to study larger prototypes. The thermal behavior of the tank is described by the local thermal non-equilibrium equations [11], which describe the heat transfer between the fluid and the packed bed (Eq. 5 and Eq. 6). The energy balance equations for the porous filler material and air can be written as:

$$(1-\varepsilon)\rho_s \cdot c_{p_s} \cdot \frac{\partial T_s}{\partial t} = (1-\varepsilon)k_s \cdot \frac{\partial^2 T_s}{\partial x^2} + h_v \cdot \left(T_f - T_s\right) \tag{5}$$

$$\varepsilon \cdot \rho_f \cdot c_{p_f} \cdot \frac{\partial T_f}{\partial t} + u \cdot \rho_f \cdot c_{p_f} \cdot \frac{\partial T_f}{\partial x} = \varepsilon \cdot k_f \cdot \frac{\partial^2 T_f}{\partial x^2} + h_v \cdot \left(T_s - T_f\right) \tag{6}$$

The Biot number is defined as the ratio of resistances due to particle conduction to the one due to convection. The solid particle temperature gradients are generally ignored when the Biot number is less than 0.1 [12].

$$Bi = \frac{h \cdot D}{2 \cdot k_s} \tag{7}$$

For the determination of the convective heat transfer in the packed bed, between the solid and the fluid, the expression of Gunn [13] is adopted as it is typically used for packed beds:

$$\frac{h \cdot D}{k_f} = \left(7 - 10 \cdot \varepsilon + 5 \cdot \varepsilon^2\right)\left(1 + 0.7 \cdot \Pr^{1/3} \cdot \mathrm{Re}_p^{0.2}\right) + \left(1.33 - 2.4 \cdot \varepsilon - 1.2 \cdot \varepsilon^2\right) \Pr^{1/3} \cdot \mathrm{Re}_p^{0.2} \tag{8}$$

With the aforementioned expressions and an assumed thermal conductivity for the 70% purity alumina balls of 15 W/m/K, the Biot number is nearly 0.02, below 0.1. For this reason, a simplified uni-dimensional mathematical model is presented, considering that the air temperature and the filler material temperature are almost the same. The energy balance equation can be written as:

$$\left(\rho \cdot c_p\right)_{eff} \cdot \frac{\partial T_f}{\partial t} + \varepsilon \cdot \left(\rho \cdot c_p\right)_f \cdot u_f \cdot \frac{\partial T_f}{\partial x} = k_{eff} \cdot \frac{\partial^2 T_f}{\partial x^2} - U \cdot a \cdot \left(T - T_{amb}\right) \tag{9}$$

To simplify the analysis, the following assumptions are made:

- The heat transfer by radiation between pebbles is not considered,
- The thermal properties of fluid and solid are kept constant within the charging/discharging process,
- The temperature of TES varies along the axial direction,
- The heat transfer coefficient though the chassis is kept constant during the storage process.

With the implementation of the differential equation in Matlab the numerical model can be run under different conditions.

4. Results

Fig. 2 represents the average temperature profile at each height during the charging process for different air mass flow rate (38-75 kg/h) for 9 mm 70 % alumina spheres. With the present placement of the thermocouples (Fig. 1), 94 % of the measurements are less than 5 % dispersion to the average value presented. The air inlet temperature for all these cases was increases progressively from ambient to a maximum of nearly 570ºC. Tests were performed until all the tank levels were under stationary state. Level 0.5 corresponds to the air inlet temperature while level 0 corresponds to the air outlet temperature.

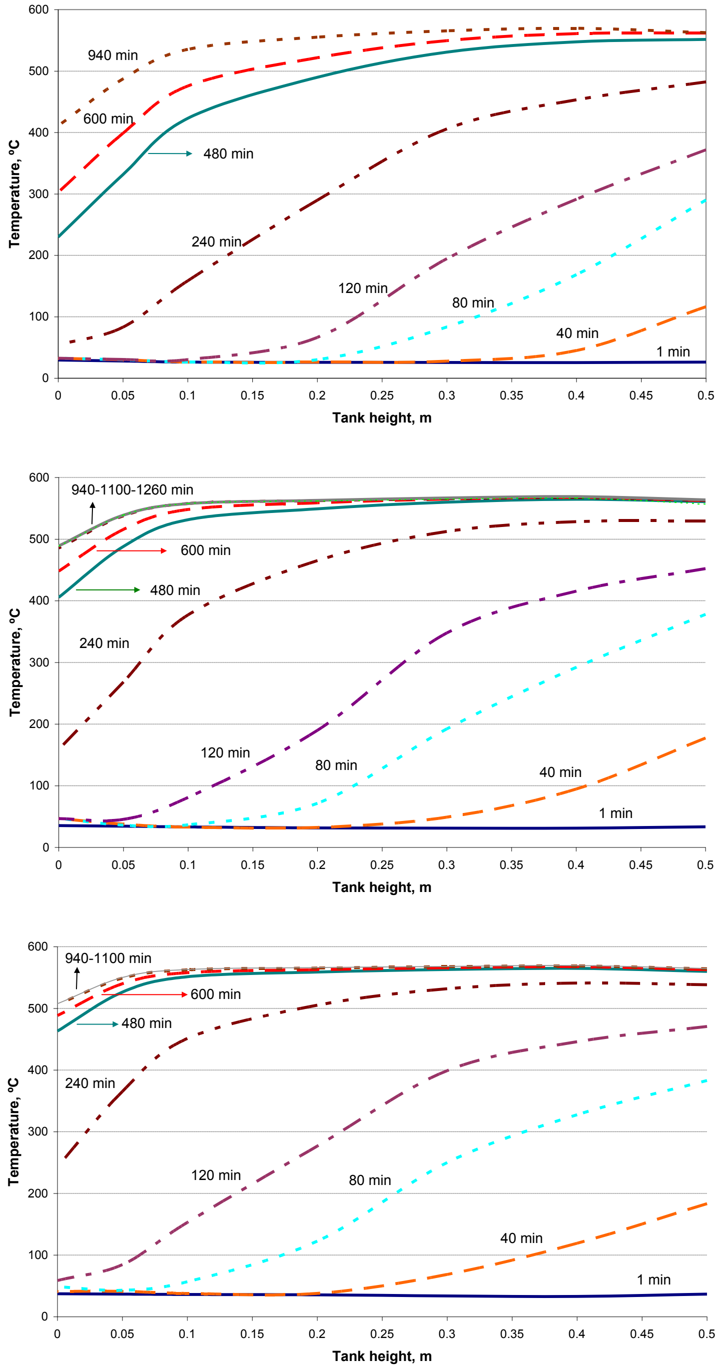
Temperature, °C
Tank height, m
940 min
600 min
480 min
240 min
120 min
80 min
40 min
1 min
Temperature, °C
Tank height, m
940-1100-1260 min
600 min
480 min
240 min
120 min
80 min
40 min
1 min
Temperature, °C
Tank height, m
940-1100 min
600 min
480 min
240 min
120 min
80 min
40 min
1 min

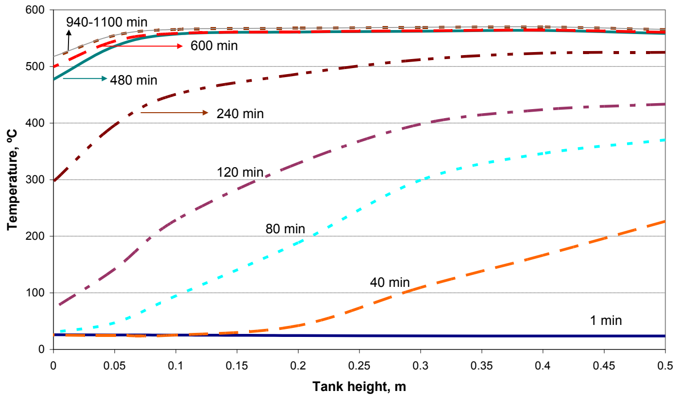

Fig. 2. Temperature profiles along tank height at different times during a charging process for: (a) first 38 kg/h, (b) second 54 kg/h, (c) third 66 kg/h, (d) fourth 75 kg/h.

The values obtained for the thermal charging efficiency, according with the eq. 4, of the test carried out are showed in the Fig. 3 and Fig. 4

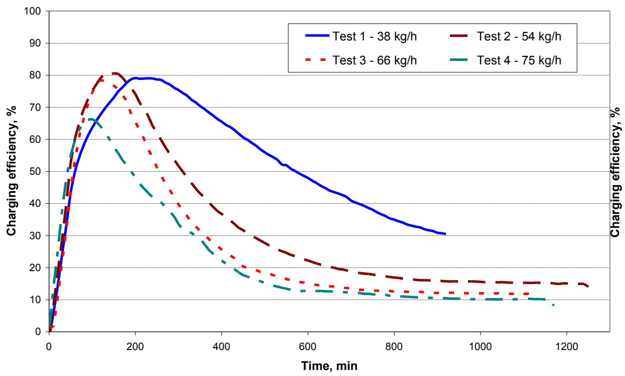

Fig. 3. Charging efficiencies for different mass flow rates with an inlet air temperature of 570 ºC

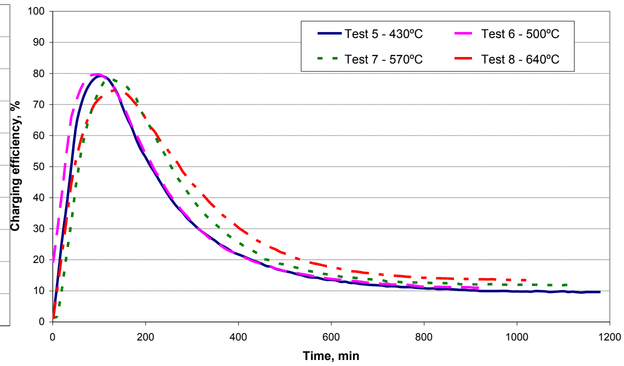

Fig. 4. Charging efficiencies for different air inlet temperature and an air mass flow rate of approximately 67 kg/h

For a maximum air inlet temperature of 570ºC and different air mass flow rates the maximum charging efficiency is 80.7% for test 2 (Fig. 3). For higher or lower values of the air mass flow rate the thermal behavior of the tank is worse, with it's explained for a poorest heat transfer through the packed bed. Specially significant are the results of test 4 with an air mass flow of 75 kg/h, where the heat transfer is very poor, reducing considerably the residence time of the HTF into the packed bed, (test 4 presents two times the velocity of test 1).

On the other hand, for an almost constant air mass flow rate, 67 kg/h, and different air inlet temperatures (430-640ºC), the maximum charging efficiency is 80.3% for test 6 (Fig. 4). Test 5 presents similar efficiency to test 6, but for higher air inlet temperature the charging efficiency decrease, mainly because of the thermal losses through the chassis of the packed bed. Table 4 shows the maximum efficiencies for the test performed.

Table 4. Maximum charging efficiency for the tests carried out

Test	1	2	3	4	5	6	7	8
Maximum charging thermal efficiency, (%)	79.2	80.7	78.6	66.4	79.5	80.3	78.6	74.7

Further experimentation is being carried out to analyze other possible materials and configurations with the aim of identifying cheaper materials and/or configurations of materials, that make TES using air as HTF a competitive option.

With the aforementioned numerical model, a comparison for test 3/7 is carried out. Fig. 5 depicts the results between experimental (exp) data of temperature distribution into the packed bed (solid line) with the numerical (numer) simulation results (dashed lines).

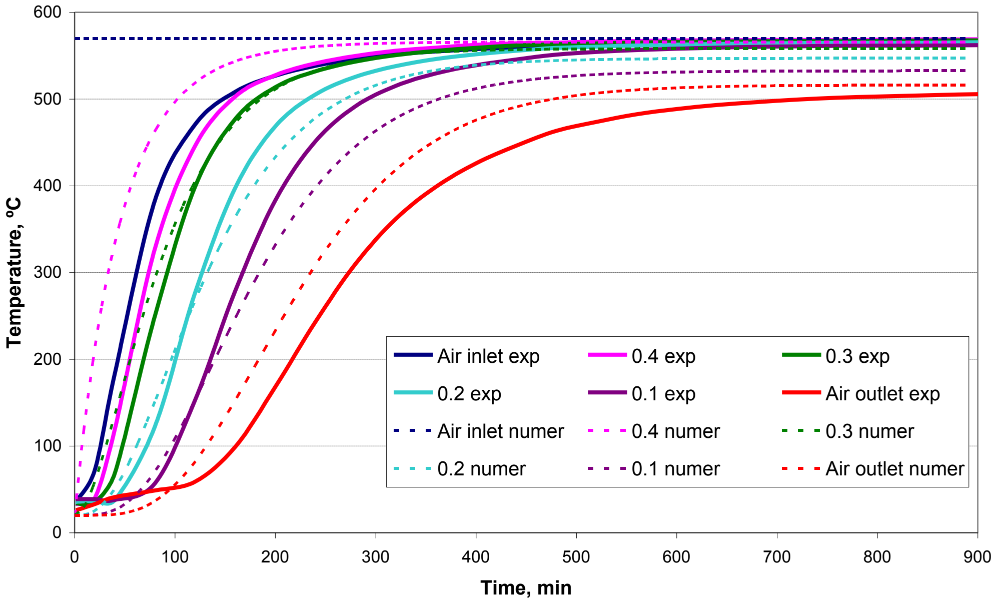

Fig. 5. Temperature profile in the packed bed, experimental (exp) and numerical (numer), during a charging process for test 3/7

The main differences between the numerical model and the experimental data are due to the assumption in the model that the air inlet temperature into the packed bed is at a constant 570°C (horizontal dash dark blue line), while in the experimental test bed the inlet air does not achieve the target temperature until minute 500 (solid dark blue line). Moreover, even though simulations results and experimental data curves are not overlapped, specially during the transient state, the temperature gradients are well described by the uni-dimensional equation.

Other reasons for which the experiment and the simulation do not match are that the thermal losses through the chassis of the storage system are kept constant (temperature independent) for the whole axial length. This simplification should not introduce much uncertainties as the thermal losses were evaluated at an average chassis temperature, but surely that the introduction of a temperature dependent convective heat transfer between the chassis and the ambient would improve the numerical estimation. Moreover, an important simplification is related to the thermal properties of the fluid and the solid, considered thermal independent. In the case of alumina, the simplification is quite acceptable, as the thermal properties presents a slight variation over the temperature range but for the air used as HTF the variation in the working range (20-600ºC) is large enough to influence over the numerical results.

5. Outlook

Due to the possibility of achieving the envisaged specific costs for the storage sub-system under 20 €/kWh$_{th}$, this paper describes a lab-scale packed bed storage system developed by Ciemat-PSA with the main objective of identifying economically competitive options on materials and geometries for regenerative heat storage using air as HTF.

First dynamic tests with 9 mm 70 % alumina spheres, have been performed to check the behavior of the TES facility during different charging strategies. Results for the packed bed under different working states have been presented. A maximum charging efficiency of 81% for 9 mm 70 % alumina spheres during the charging process occur for an air inlet temperature of 570ºC and an air mass flow rate of 54 kg/h. One of the objectives of the facility is to study cheaper materials with moderate energy densities, to analyze the compromise between the material cost and store energy, with the objective of find economical solutions for future plant developments.

Furthermore, a numerical model has been described and checked with the experimental results. Some discrepancies are observed and justified. The main necessaries improvements are due to the fluid thermal properties and the thermal losses through the chassis that should be considered temperature-dependent. Moreover, the radiative heat transfer mechanisms have to be implemented, due to the high working temperatures, which should increase the model confidence.

Future works will study deeply the influence of the radial component, discharging strategies and the remaining filler material and will present transient calculation with no air flow to determine how long the thermocline can be maintained.

Acknowledgements

The author wish to thank “Comunidad de Madrid” and “European Social Fund” for its financial support to the SOLGEMAC Project through the Programme of Activities between Research Groups (S2009/ENE-1617). The author wishes to acknowledge Ms. M.A. Martinez Tarifa for her many helpful comments and support.

References

[1] Avila-Marin AL. Volumetric receivers in solar thermal power plants with central receiver system technology: a review. Solar Energy 2001; 85: 891–910.
[2] Fricker HW. PHOEBUS phase 1B executive summary. 1990, CH 5232 Villigen-PSI.
[3] Zunft S, et al. High-temperature heat storage for air-cooled solar central receiver plants: A design study. 15th SolarPACES Symposium, Berlin, Germany, 2009.
[4] Hennecke K, et al. Solar power tower Jülich. First test and demonstration plant for open volumetric receiver technology in Germany. 14th SolarPACES Symposium, Las Vegas, USA, 2008.
[5] Gil A. State of the art on high temperature thermal energy storage for power generation. Part 1—Concepts, materials and modellization. Renewable and Sustainable Energy Reviews 2010; 14: 31-55.
[6] Khare S, et al. Selection of materials for high temperature sensible energy storage. Solar Energy Materials & SolarCells 2013; 115: 114–122.
[7] Avila-Marin, AL, et al. Lab-scale characterization of heat storage solutions for concentrated solar power with open volumetric central receiver technologies. 18th SolarPACES Symposium, Marrakech, Morocco, 2012.
[8] Kolb J, et al. Power Tower Technology Roadmap and Cost Reduction Plan. 2011, Report Nº. SAND 2011-2419.
[9] Fricker HW. Regenerative thermal storage in atmospheric air system solar power plants. Energy 2004; 29: 871–881.
[10] Zavattoni SA, et al. Effective Thermal Conductivity and Axial Porosity Distribution of a rock-bed TES system: CFD modeling and experimental validation. 18th SolarPACES Symposium, Marrakech, Morocco, 2012.
[11] Xiaoping Y, et al. Criteria for performance improvement of a molten salt thermocline storage system. Applied Thermal Engineering, 2012; 48: 24-31.
[12] Mills AF. Heat Transfer, 2nd edition, Prentice Hall, Upper Saddle River New, Jersey; 1999.
[13] Gunn DJ. Transfer of heat or mass to particles in fixed or fluidized beds. International Journal for Heat and Mass Transfer 1978; 21:467-476.